# ATOMIZATION CHARACTERISTICS OF HIGH-SPEED ROTARY BELL ATOMIZERS

J. Domnick*, M. Thieme
Institut für Industrielle Fertigung und Fabrikbetrieb (IFF)
Universität Stuttgart, Nobelstr. 12, D-70569 Stuttgart, Germany
Tel. +49 711 970 1762, Fax. +49 711 970 1035
e-mail: jhd@ipa.fhg.de

**Abstract**

High-speed rotary bell atomizers are widely used in the painting industry for high quality applications. They provide a highly uniform film thickness with reasonable transfer efficiency due to the additional electrostatic field supporting the droplet transport towards the target. A basic requirement for this type of paint atomizers consists in a fine and reproducible atomization of a large variety of different paints, ranging from solvent-based materials to highly non-Newtonian water-borne systems. Furthermore, a broad range of paint flow rates must be covered.

The present contribution summarizes the results related to the atomization of Newtonian fluids with high-speed rotary bells. Water-sucrose-alcohol solutions have been used to vary viscosity and surface tension independently. A design of experiments (DOE) scheme has been applied.

The atomization processes observed could be divided into two distinct modes, i.e., jet disintegration and turbulent disintegration, the latter one being characterized by the presence of both radial and lateral fluid structures close to the bell edge. The separation line between these modes is expressed in terms of the *We*-number and the flow number *q*. For jet disintegration, the Sauter diameter has been found to be a function of the three dimensionless parameters *Re*-number, *We*-number and the flow number *q*. In turbulent disintegration, the Sauter diameter is a function of the *We*-number only. Finally, measured size distributions have been fitted by the 3-parameter log-hyperbolic function and location and shape of the distributions discussed as functions of the dimensionless parameters. Compared to other types of atomizers, it was found that the size distributions are not particularly narrow as expected from the well organized disintegration pattern especially in the jet mode.

In the future, the investigations will be extended to non-Newtonian liquids, such as various low concentration polymer solutions that also exhibit viscoelastic effects.

## Introduction

High quality painting represents a challenging task for the development and practical use of atomizers. Many important properties of the produced paint film, e.g., colour, metallic effect, levelling, or gloss are directly related to the characteristics of the spray that is produced by the atomizer. The most evident case are very large droplets that do not level out after impact on the surface.

In general, some work has already been done to examine the atomization of rotary atomizers, and basic information may be found, e.g., in [1], [2], and [3], however, there are only a few publications dealing with cup-shaped rotary atomizers with small diameters and very high rotational speeds, as specifically used in the painting industry. Recently, *Corbeels et al.* [4] have presented results for a high-speed rotary atomizer used for painting applications, applying a Malvern particle sizer to investigate the effect of operating conditions and liquid properties on the atomization performance. These results may be used for comparative purposes, however, only five different fluids have been considered. Furthermore, the *Rosin-Rammler* distribution has been used to discuss variations in the shape of the size distribution, which was found to give only a limited fitting quality to measured distributions. No comparisons between experimental and fitted distributions are shown.

* corresponding author

*Scholz* [5] has also investigated a specific high-speed rotary bell used for painting purposes. Unfortunately, only water has been used for atomization while focussing on the influence of the application parameters on the disintegration process and the droplet size distributions. For droplet size measurements, both Fraunhofer diffraction and phase-Doppler anemometry have been applied. According to *Scholz*, the atomizer works purely in the jet disintegration mode. Only at rather low rotating speeds around 10000 1/min some first fragments of sheets have been observed. For the characterization of the droplet mean diameters in jet mode, a modified *Dombrowski and Lloyd* [6] equation has been proposed.

**High-speed rotary bell investigated**

The investigations shown here were made with a state-of-the-art high-speed rotary bell atomizer (Dürr Systems GmbH) used in automated paint applications. A front view of the atomizer is depicted in Fig. 1. In contrast to other rotary atomizers, high-speed rotary bells are designed to generate variable spray cone widths and high transfer efficiencies. The spray cone width is adjusted through the bell speed and a so-called shaping air, emerging from a ring of nozzles behind the bell and directing a well defined air flow along the outer surface of the rotating bell. At the bell edge, the axial velocity of the shaping air has been measured to be around 20 to 30 m/s. In addition, high-voltage up to 70 kV is applied to the bell, directly charging the droplets and creating an additional force on the droplets directing them to the grounded target. In this way, the transfer efficiency, i.e., the solid mass fraction of atomized paint that actually reaches the target, may exceed 90 % when using a large flat plate as target.

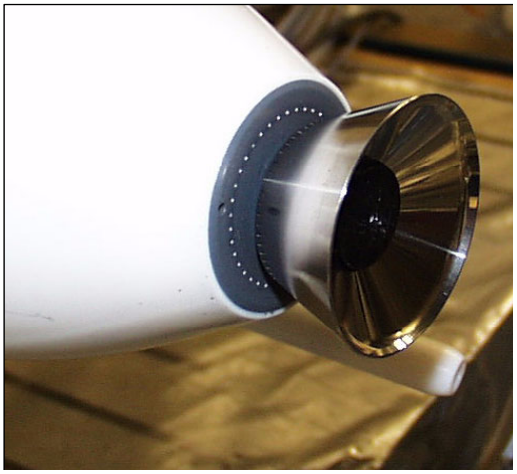

**Fig. 1**: High-speed rotary bell (Dürr Systems GmbH)

In Table 1, the major characteristics of the atomizer and the operating conditions investigated are summarized. The bell used in the present investigations has a diameter of 55 mm and is specifically adapted to water-borne systems. The liquid is delivered by a narrow annular shaped slit formed by the bell surface and an inner disk of approximately 25 mm diameter. The purpose of this slit is to form an initial stable fluid film on the bell, and to prevent the formation of ligaments on the bell surface that would reduce the atomization quality [7]. Also, the shape of the inner bell surface has been purposely designed to keep the fluid film stable. The bell surface is basically divided into two different sections: While the inner part has a constant flow angle, the outer part shows a decreasing angle with respect to the bell axis to increase the normal component of the centrifugal volume force acting on the film, thereby stabilizing the film. The edge speed of the bell varies between 28 m/s at 10000 1/min and 172 m/s at 60000 1/min. Due to this high speed and the need to keep vibrations as small as possible, a powerful air bearing is used.

| | |
|---|---|
| **Bell diameter** | 55 mm (no serrations) |
| **Bell material** | Stainless steel |
| **Liquid flow rate** | 50 - 250 ml/min |
| **Bell speed** | 10000 - 60000 1/min |
| **Bell edge velocity** | 28 - 172 m/s |

**Tab. 1**: Atomizer characteristics

**Experimental set-up and measuring techniques**

As the future tests are planned with real water-based paints, the experiments had to be conducted in a closed spray booth equipped with a full air condition system and constant downdraft air velocity of approximately 0.3 m/s. In order to also allow experiments with high voltage applied, a special traversing system for the atomizer had to be designed with all major parts close to the atomizer being made of non-conductive material. Both the atomizer and the target were fixed to the traversing system, enabling a 3-component positioning with a precision better than $\pm 0.5$ mm. All optical measuring units were mounted on fixed frames.

Two major optical measuring techniques were used to investigate the atomization of the high-speed rotary bells considered. For qualitative purposes, images of the liquid disintegration process at the bell edge were made using a Nanolight 18 ns flash and a video camera in a standard inline arrangement. The Nanolight performance was enhanced by a special imaging system, applying a large Fresnel lens to increase the size of the spot. The flash was synchronized with the video camera yielding a frame rate of 25 1/s. The short exposure time of the flash delivers 'frozen' images of the disintegration process even at the highest bell speeds, a frame-to-frame identification of fluid ligaments or droplets is not

possible, however. As typical droplet diameters are in the range of 30 µm and below, this set-up was found to be a good compromise between speed and frame resolution.

Quantitative droplet size measurements were made with a Malvern Spraytec Fraunhofer type particle sizer, yielding a 400 µm size range with a 200 mm receiving lens. The measuring volume of the Spraytec, having a diameter of 9 mm, was positioned at a distance of approximately 10 mm from the bell edge to be able to detect the true droplet production of the atomizer. This is of specific importance as Fraunhofer diffraction instruments measure a concentration weighted size distribution that is affected by the presence of size/velocity correlations. On the other hand, the visualizations indicate the formation of the final droplet size distribution just a few millimeters away from the bell edge. An identical measurement set-up has already been used by *Corbeels et al*. [4].

**Test fluids and test conditions**

In order to change surface tension and viscosity independently, other components have to be added to the water. For experimental usage such additives should not be harmful, poisonous or highly corrosive. According to *Wolf* [8], non-Newtonian effects can be avoided using alcohol-water mixtures for surface tension reduction. Furthermore, *Wolf* found a linear relationship between alcohol concentration and surface tension for methanol- and ethanol-water mixtures, whereas for higher order alcohols a deviation from this linear behaviour could be observed. Considering these results and the harmfulness of methanol, ethanol-water mixtures have been chosen to vary the surface tension of the test liquids.

The viscosity of these ethanol-water mixtures can be varied by adding either glycerine or sucrose. Glycerine has a stronger influence on the surface tension, therefore, sucrose was chosen. Finally, surface tension variations between 27 and 75 mN/m could be realized, while the viscosity could be varied by a factor of 40 from water viscosity up to 40 mPa·s. The composition of the test fluids basically follows the recommendations of *Dorfner et. al* [9] for pressure swirl atomization. The final properties of the 25 different solutions used in the present investigation are shown Fig. 2. The variations of the density were less than 25 % and therefore neglected. For each mixture, the viscosity was measured by a Couette-type rotational viscometer (PHYSICA UDS 200). The surface tension was determined with a drop tensiometer by DATA PHYSICS.

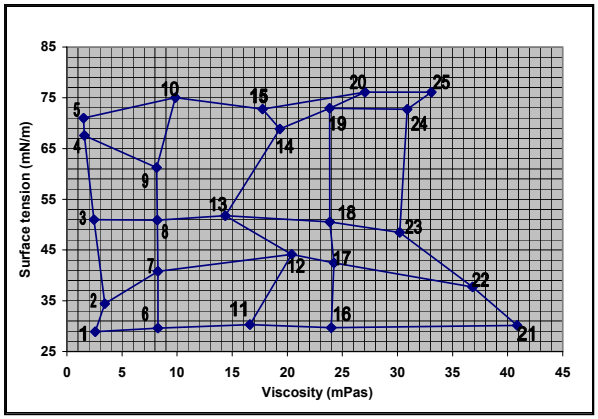


**Fig. 2**: Viscosity and surface tension of the test fluids

A design of experiments program [10] has been applied to derive homogeneously distributed test conditions within the operating and fluid property ranges considered. In total, 66 experiments were performed, changing bell speed, fluid flow rate, viscosity and surface tension. Based on the application parameters of the atomizer and the fluid properties, three different dimensionless numbers are derived, i.e., *Re*-, *We*- and the flow number *q*. For rotary atomizers, the following definitions apply:

$$Re = \frac{\pi D^2 n}{\nu_L}, \quad We = \frac{\pi^2 D^3 n^2 \rho_L}{\sigma}, \quad q = \sqrt{\frac{2\rho_L}{\sigma \cdot D}} \cdot \frac{\dot{V}}{\pi \cdot D}$$

In terms of the dimensionless numbers the following range has been investigated:

| | |
|---|---|
| *Re*-number: | $4.5 \cdot 10^4 - 6.6 \cdot 10^6$ |
| *We*-number: | $6.7 \cdot 10^5 - 6.6 \cdot 10^7$ |
| Flow number *q*: | $2.5 \cdot 10^{-3} - 2.2 \cdot 10^{-2}$ |

It should be emphasized that the measurements reported in this paper have been performed without high voltage being applied to the bell. Therefore, the results are valid for externally charging rotary atomizers as well where the charging of the droplets is achieved through the interaction with free ions emerging from electrodes at a distance of approximately 75 mm from the bell edge. The influence of the shaping air on the disintegration process and, hence, on the resulting droplet size distributions has not been taken into consideration. As shown below, disintegration takes place in a very narrow region around the bell edge where the velocity field of the air is mainly dominated by the rotation of the bell. Numerical simulations have shown that the mean axial air velocity in this region is around 20 m/s and therefore significantly smaller than the tangential velocity depending on the bell speed only. This is consistent with the results of

*Scholz* [5], who could observe only a weak and statistically insignificant effect of the shaping air on the mean droplet diameter.

**Characterization of the disintegration process**

Using the Nanolight flash, the disintegration process has been visualized. For the 55 mm diameter bell, the frame width has been chosen to be around 4-5 mm to be able to characterize the overall disintegration structure while still being able to identify the properties of a single jet leaving the bell edge. Typical disintegration processes observed at different liquid flow rates at a bell speed of 10000 1/min are shown in Fig. 3.

In jet mode, liquid jets with usually well defined diameter and spacing emerge from the bell edge. Depending on the operating conditions, the jet diameters vary between 15 and 50 µm. Using water, maximum jet lengths were found to be around 200 µm at a liquid flow rate of 100 ml/min and a speed of 40000 1/min. Corresponding jet diameters close to the origin at the bell edge were around 40 µm. As expected, the length of the jets increases with increasing fluid viscosity resulting in two counter current effects: On the one hand, viscosity hinders the disintegration of the jets into droplets, on the other hand the elongated jets usually have smaller diameters at the point of break-up. Consequently, only a weak dependency of the droplet mean diameters on *Re*-number has been found as shown below.

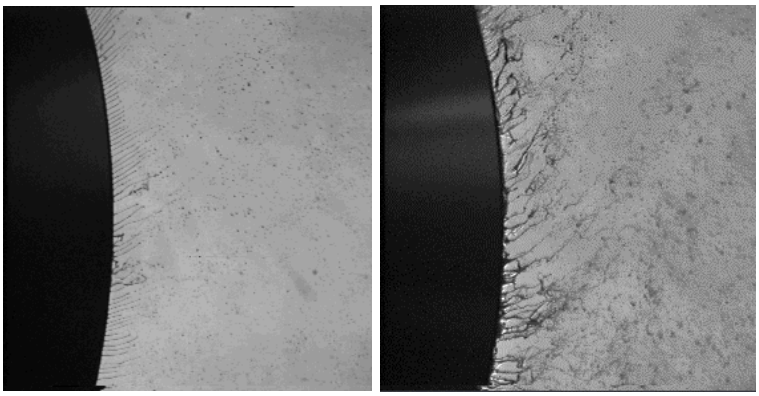

**Fig. 3**: Jet disintegration at 100 ml/min (left) and turbulent disintegration at 600 ml/min (right) at a bell speed of 10000 1/min

At larger liquid volume flow rates, the disintegration process changes, and more and more lateral fluid structures, sometimes 'bridges' between jets can be observed as they detach from the bell edge. Although in some regions individual radial jets can still be identified, the disintegration process in total becomes less organized. The lateral structures may be considered as the result of a partial local sheet break-up taking place very close to the bell edge. This process is further referred to as turbulent disintegration mode. These disintegration patterns have also been observed by *Scholz* [5], still classifying them as jet mode, however.

In Fig. 4, the observed disintegration patterns are shown as a function of flow number and *We*-number. This graph was found to give the most appropriate separation between jet and turbulent disintegration. Consequently, an equation for a critical flow number $q_{crit}$ can be derived being a function of the *We*-number only:

$$q_{crit} = 0.0034 \ln(We) - 0.0404$$

If $q$ is larger than $q_{crit}$ for the given *We*-number, the atomizer is operating in turbulent mode. This result is consistent with the approach of *Hege* [11], who defined an optimum flow rate which, apart from the mechanical parameters (bell speed and diameter), depends only on the surface tension of the liquid and is independent of the *Re*-number.

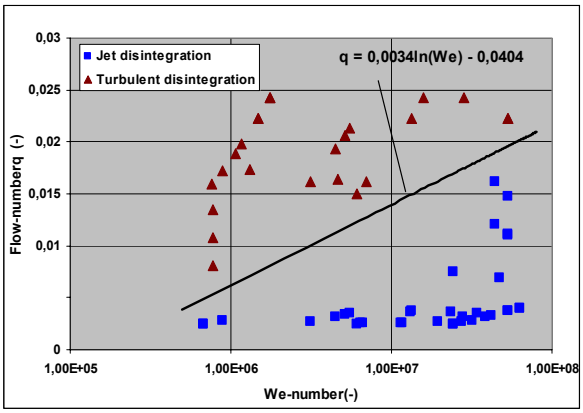


**Fig. 4**: Separation between jet and turbulent disintegration mode

With respect to numerical simulations of the spray coating process [12], it is important to note that the disintegration process is completed within a few millimeters from the bell edge. Hence, initial conditions for the droplets may be taken from size measurements at this location. Also, it can be concluded that the initial conditions of the droplets are symmetric with respect to the atomizer axis, which implies an important simplification for the numerical simulations.

**Mean droplet diameters**

In the following, the results of the Fraunhofer diffraction measurements are discussed. Mainly the Sauter mean diameter $D_{32}$ has been used to verify the influence of the fluid properties and the operating conditions on the characteristics of the droplet size distributions.

Of course, the identified different disintegration modes have to be treated separately. For both cases, empirical correlations for the Sauter mean diameter as a function of the dimensionless parameters have been derived. The resulting equations are:

Jet disintegration:

$$D_{32} = 0.60 \cdot Re^{0.056} \cdot We^{-0.58} \cdot q^{0.41} \qquad R = 0.93$$

Turbulent disintegration:

$$D_{32} = 0.034 \cdot We^{-0.47} \qquad R = 0.79$$

Comparisons between measured and calculated Sauter mean diameters are depicted in Fig. 5. For jet disintegration, a correlation factor $R$ of 0.93 is obtained, indicating firstly an excellent agreement between measurement and calculation. Secondly, this is also an indication for a rather high regularity of the underlying disintegration process of nicely separated liquid jets into droplets.

As can already be expected from the visualization images, the turbulent disintegration is much less organized. The disintegration patterns of the sheets and jets vary strongly from image to image and even within a single image. This process is dominated by the local properties of the film itself and the surrounding air flow field. There is no information available with respect to mechanical influences on the droplet formation process, e.g., vibrations of the rotating bell which might have an additional, to some extent, random effect.

For the case of turbulent disintegration, the measured mean droplet diameters are independent of the *Re*-number. This has already been found by *Corbeels et al.* [4] for a 70 mm diameter bell at bell speeds above 20000 1/min.

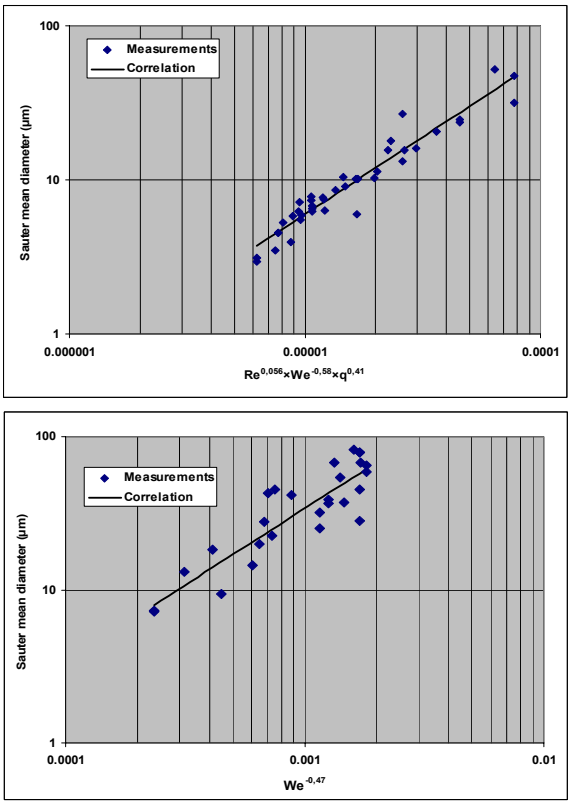


**Fig. 5**: Obtained correlation for the jet (top) and turbulent (bottom) disintegration mode

A further analysis of the disintegration process may be performed by considering the liquid film thicknesses at the bell edge which can be calculated from the following equation given by *Hinze and Milborn* [13]:

$$\delta = \sqrt[3]{\frac{3\nu_L \dot{V}}{2\pi^3 D^2 n^2 \sin\beta}}$$

As shown in Fig. 6, The theoretical film thicknesses vary between approximately 70 µm at low *Re*-numbers and less than 5 µm at high *Re*-numbers. Of course, the calculation does assume an evenly distributed liquid film on the bell surface. This could be confirmed by the Nanolight images in which no indication for a local dry out of the bell surface was found.

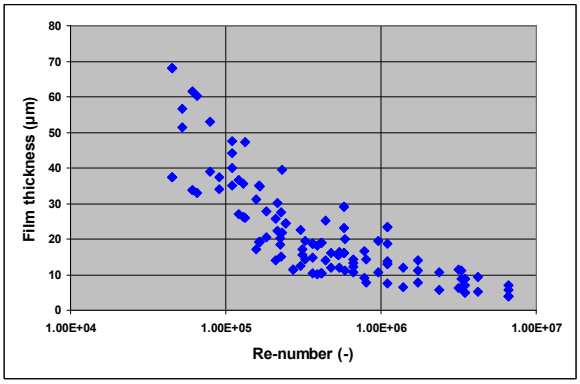


**Fig. 6**: Calculated film thickness at the bell edge as a function of the *Re*-number

Using the film thicknesses, the atomization can be expressed in terms of the dimensionless Sauter mean diameter $D_{32}/\delta$ which itself may be again correlated with the other dimensionless parameters. The resulting functions are:

Jet disintegration:

$$D_{32}/\delta = 3.7 \cdot Re^{0.38} \cdot We^{-0.40} \qquad R = 0.92$$

Turbulent disintegration:

$$D_{32}/\delta = 2.9 \cdot Re^{0.32} \cdot We^{-0.34} \qquad R = 0.64$$

In these cases, the effect of the flow number $q$ can be neglected.

**Further characterization of the droplet size distributions**

So far, the measured size distributions have been discussed in terms of mean diameters only. A further characterization may be performed by applying mathematical distribution functions to the size distributions. For rotary atomizers, *Corbeels et al.* [4] used the well-known *Rosin-Rammler* distribution to characterize mean and width of the measured size distributions. In the present investigations, however, it was found that the 3-parameter log-hyperbolic distribution provides an appropriate representation of the obtained size distributions. This distribution is a subset of the 4-parameter log-hyperbolic function which was initially introduced by *Barndorff-Nielsen* [14], and later on applied to sprays by *Bhatia et al*. [15]. As shown in Fig. 7, the 3-parameter log-hyperbolic distribution includes the parameters μ, θ and *a*, which have certain geometrical meanings. μ is a location parameter defining the mean size of the distribution, θ is the angle of the hyperbola axis relative to the coordinate system defining the skewness of the distribution, and *a* the slope of the asymptotes of the hyperbola which is equivalent to the width of the defining size distribution [16]. A rotation of θ in counter clockwise direction (negative θ) induces a positive skewness, i.e., the distribution will have a longer tail towards larger particles. Using the three parameters, the original form of the size distribution can be reconstructed, and changes in the shape of the distribution can be deduced thus giving insight into the physical processes involved.

In Fig. 8, sample fits of the volume weighted size distributions measured in the tests # 36, 15 and 37, purposely representing a large variation of the dimensionless parameters, are depicted. In all three cases, purposely selected to cover on the one hand an almost log-normal shaped distribution at a low flow number in jet mode as well as on the other hand a highly skewed distribution at a high flow number in turbulent mode, the representation of the measured size distributions is very good.

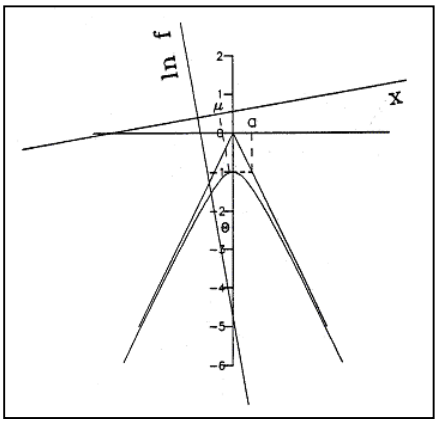


**Fig. 7**: Shape of the 3-parameter log-hyperbolic function

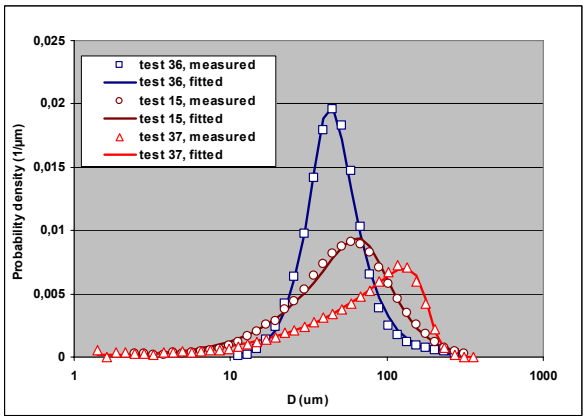


**Fig. 8**: Reconstructed measured and fitted size distributions

One could assume that the size distributions obtained in the turbulent disintegration mode are generally broader which, however, is not the case. In Fig. 9, the three parameters of the log-hyperbolic function are shown as a function of the *We*-number, which according to the correlations above should reveal the most significant effects. From these figures, the following conclusions can be drawn:

1. The size parameter μ decreases with increasing *We*-number, which is consistent with the correlations for the Sauter mean diameter. A slight tendency for a larger μ-values at similar *We*-numbers for turbulent disintegration mode compared to jet mode can be observed.

2. There is no significant correlation between the parameter θ, i.e., the skewness of the distribution, and the *We*-number

3. The parameter *a* increases with increasing *We*-number. To some extent, this reflects the observation of a less homogeneous disintegration process at higher rotational speed. *Corbeels et al*. [4] also attributed this effect to

the increased action of aerodynamical forces on the local disintegration of the ligaments. In the present investigations, no significant difference between the jet and turbulent disintegration modes has been found.

As already pointed out by *Corbeels et al.* [4], the size distributions of the high-speed rotary bell atomizers are not particularly narrow, as one might expect especially in the jet mode with its well-organized disintegration process.

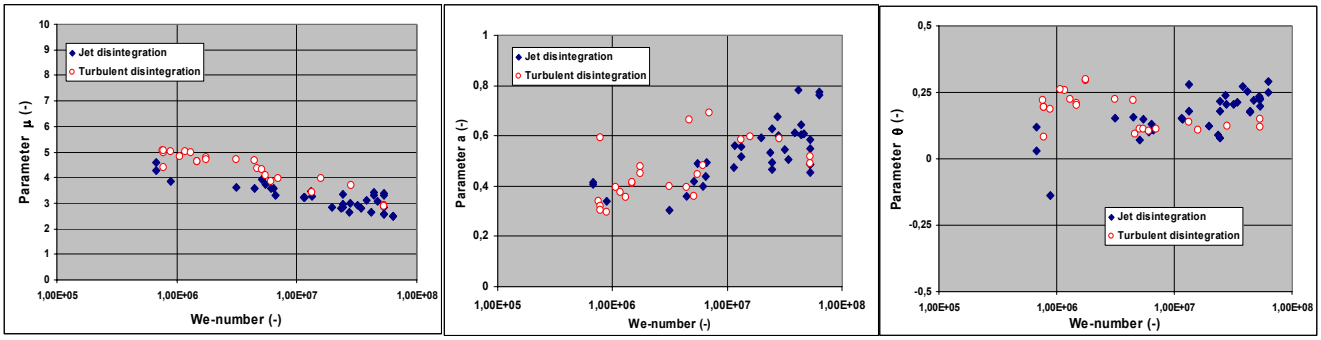


**Fig. 9**: Parameter μ (left), *a* (center) and θ (right) of the 3-p log-hyperbolic distribution as a function of the *We*-number

**Summary and outlook**

The present contribution deals with the atomization process of a rotary atomizer applied mainly in painting processes. Compared to other rotary atomizers used, e.g., in spray drying or powder production, this type of atomizer is characterized by a small bell diameter (typically between 20 and 70 mm) and very high bell speeds up to 70000 1/min. Consequently, the ranges of the *Re*- and *We*-numbers considered herein are mostly higher than those in former investigations, e.g., [6], [11] and [17].

The atomization processes observed for this type of atomizer can be divided into two distinct modes, i.e., jet disintegration and turbulent disintegration, the latter one being characterized by the presence of both radial and lateral fluid structures close to the bell edge. The separation line between these two modes is expressed in terms of the *We*-number and the flow number *q,* and, hence, independent of the *Re*-number.

The atomization results have been represented in terms of the Sauter mean diameter. For jet disintegration, the Sauter diameter has been found to be a function of the three dimensionless parameters *Re*-number, *We*-number and the flow number *q*. In turbulent disintegration, the Sauter diameter is a function of the *We*-number only, implying that mainly aerodynamic forces that act on the liquid agglomerations leaving the bell edge are important for the disintegration process.

Finally, measured size distributions have been fitted by the 3-parameter log-hyperbolic function, and its parameters were expressed as a function of the dimensionless parameters. It has been shown that the width of the size distributions increases with increasing *We*-number, however, no significant differences between jet and turbulent disintegration could be observed. Compared to other types of atomizers, the size distributions are not particularly as narrow as one might expect from the well-organized disintegration pattern in the jet mode.

Future investigations will be extended to non-Newtonian liquids, such as various low concentration polymer solutions that also exhibit viscoelastic effects.

**Acknowledgements**

The present work has been supported by the Deutsche Forschungsgemeinschaft through grant No. Do 251/10-1 and 2. This support is gratefully acknowledged by the authors.

**Nomenclature**

| | | |
|---|---|---|
| $a$ | width parameter of the 3-p log hyperbolic function | (-) |
| $d^*$ | non-dimensional size parameter | (-) |
| $D$ | bell diameter | m |
| $n$ | bell speed | 1/min |
| $q$ | dimensionless flow number | (-) |
| $Re$ | *Reynolds*-number | (-) |
| $\dot{V}$ | liquid flow rate | m³/s |

| | | |
|---|---|---|
| *We* | *Weber*-number | (-) |
| $\beta$ | bell surface angle | (°) |
| $\delta$ | film thickness at the bell edge | (m) |
| $\theta$ | skewness parameter of the 3-p log hyperbolic f. | (-) |
| $\mu$ | size parameter of the 3-p log hyperbolic function | (-) |
| $\mu_L$ | liquid viscosity | Pa·s |
| $\nu_L$ | kinematic liquid viscosity | $m^2/s$ |
| $\rho_L$ | liquid density | $kg/m^3$ |
| $\sigma$ | surface tension | N/m |

**References**


[1] Bayvel, L., Orzechowski, Z.: *Liquid Atomization*. Bristol: Taylor & Francis, 1993.

[2] Lefebvre, A.H.: *Atomization and Sprays*. New York: Hemisphere Publishing Cooperation, 1989.

[3] Walzel, P.: Zerstäuben von Flüssigkeiten. Chem.-Ing.-Tech. 62, Nr.12, 1990, S. 983 - 994.

[4] Corbeels, P.L., Senser, D.W., Lefebvre, A.H.: Atomization characteristics of a high-speed rotary-bell paint applicator, Atomization and Sprays, Vol. 2, pp. 87-99, 1992.

[5] Scholz, T.: Experimentelle Untersuchungen zur Mehrphasenströmung im Sprühkegel eines elektrostatisch unterstützten Hochrotationszerstäubers. Progress reports VDI, Series 7: Strömungstechnik, Nr. 346, VDI-Verlag, Düsseldorf, 1998.

[6] Dombrowski, N., Lloyd, T.L.: Atomization of liquids by spinning cups, Chem. Eng. J, 8, 1974.

[7] Mehrhardt, E.: Zerstäubung von Flüssigkeiten mit rotierenden Scheiben: Flüssigkeitsauflösung, Tropfengrößen und Tropfengrößenverteilungen. Dissertation, Technical University of Berlin, 1978.

[8] Wolf, K.L., **Physik und Chemie der Grenzflächen**, Volume 2, Springer-Verlag, Berlin-Göttingen-Heidelberg, 1959.

[9] Dorfner, V., Domnick, J., Durst, F., Köhler, R.: Viscosity and surface tension effects in pressure swirl atomization, Atomization & Sprays, Vol. 5, No. 3, 1995.

[10] Visual-Xsel $2000^{XT}$ DoE, Programmbeschreibung, www.visual-xsel.com

[11] Hege, H.: Flüssigkeitsauflösung durch Schleuderscheiben, Chemie-Ing.-Techn. 36, 1964.

[12] Domnick, J., Scheibe, A., Ye, Q.: The electrostatic spray painting process with high-speed rotary bell atomizers: Influences of operating conditions and target geometries, $9^{th}$ Int. Conference on Liquid Atomization and Spray Systems, July 2003, Sorrento, Italy.

[13] Hinze, J.O., Milborn, H.: Atomization of liquids by means of a rotating cup, Journal Appl. Mech. 17, 1950.

[14] Barndorf-Nielsen, O.: Exponentially decreasing distributions for the logarithm of particle size, Proc. R. Soc. Lond. A. 353 (1977), 401-419.

[15] Bhatia, J.C., Domnick, J., Durst, F., Tropea, C.: Phase-Doppler anemometry and the log-hyperbolic distribution applied to liquid sprays, Part. & Part. Syst. Charact. 5 (1988) 153-164.

[16] Xu, T., Durst, F., Tropea, C.: The three parameter log-hyperbolic distribution and its application to particle sizing, Int. Conf. Liq. Atom. And Spray Syst. ICLASS 91, Gaithersburg, U.S.A.

[17] Fraser, R.P., Dombrowski, N., Routley, J.H.: The filming of liquids by spinning cups, Chem. Eng. Sc., 18, 1963.